Published in final edited form as:
J Med Virol. 2002 June ; 67(2): 171–186.

Hemorrhagic Fever Occurs After Intravenous, But Not After Intragastric, Inoculation of Rhesus Macaques With Lymphocytic Choriomeningitis Virus

Igor S. Lukashevich[1], **Mahmoud Djavani**[1], **Juan D. Rodas**[1], **Juan C. Zapata**[1], **Amy Usborne**[2], **Carol Emerson**[2], **Jacque Mitchen**[2], **Peter B. Jahrling**[3], and **Maria S. Salvato**[1,2,*]

[1]*Institute of Human Virology, University of Maryland, Biotech Center, Baltimore, Maryland* [2]*Wisconsin Regional Primate Research Center, Madison, Wisconsin* [3]*USAMRIID, Fort Detrick, Frederick, Maryland*

Abstract

Arenaviruses can cause hemorrhagic fever and death in primates and guinea pigs, but these viruses are not highly pathogenic for most rodent carriers. In the United States, arenaviruses precipitated outbreaks of hepatitis in captive monkeys, and they present an emerging health threat in the tropical areas of Africa and South America. We describe infection of rhesus macaques with the prototype arenavirus, lymphocytic choriome-ningitis virus (LCMV), using the WE strain that has been known to cause both encephalopathy and multifocal hemorrhage. Five macaques were inoculated: two by the intravenous (i.v.) and three by the intragastric (i.g.) route. Whereas the two i.v.-inoculated monkeys developed signs and lesions consistent with fatal hemorrhagic fever, the i.g.-inoculated monkeys had an attenuated infection with no disease. Pathological signs of the primate i.v. infection differ significantly from guinea pig arenavirus infections and make this a superior model for human viral hemorrhagic disease.

Keywords

arenavirus; mucosal infection; primates; vascular pathology

INTRODUCTION

Rodent-borne arenaviruses are a health threat to human beings who come in contact with infectious rodent excreta. Lassa fever and the South American hemorrhagic fever viruses (Old World and New World arenaviruses, respectively) account for almost one-half million cases of disease worldwide, with approximately 16% mortality [McCormick, 1990]. Lymphocytic choriomeningitis virus (LCMV), an arenavirus found in wild and domesticated rodents in the United States, was identified as the etiologic agent of fatal hepatitis in zoo-kept tamarins and marmosets [Montali et al., 1993, 1995] and as an underdiagnosed fetal teratogen in human beings [Barton and Mets, 2001]. Little is known about the routes of infection that lead to disease. We describe an experimental model for arenavirus hemorrhagic fever in which we compared the outcomes for two different routes of infection.

*Correspondence to: Maria S. Salvato, Institute of Human Virology, University of Maryland, Biotech Center, 725 West Lombard Street, Baltimore, MD 21201. E-mail: salvato@umbi.umd.edu.

The first two authors contributed equally to this work.

Animal model studies of arenavirus infection frequently employ intravenous inoculation to achieve rapid outcomes [Armstrong and Lillie, 1934; Salvato and Rai, 1996]. However, epidemiological and laboratory studies implicate mucosal routes of infection as the most common natural mode of transmission [Danes et al., 1963; Stephensen et al., 1984; ter Meulen et al., 1996; Rai et al., 1997]. Our work in the murine model of LCMV indicates that intragastric infection is less efficient than intravenous infection [Rai et al., 1996]. Although mucosal inoculation of primates via aerosol has been described [Danes et al., 1963], intragastric inoculation of primates with arenavirus has not. This represents a significant gap in our knowledge of arena-virus transmission, as one outbreak was traced to a single feeding of captive primates with LCMV-infected mice [Montali et al., 1993]. In addition, the use of rodents as a food source is a risk factor for Lassa virus seropositivity [ter Meulen et al., 1996]. We employ a rhesus macaque model, which is reportedly more similar to man in pathology than the cynomolgus macaque model [Danes et al., 1963]. We also employ the LCMV-WE strain that is known to cause fatal hemorrhagic fever when transmitted by aerosol to monkeys [Danes et al., 1963] or by intravenous inoculation to monkeys and guinea pigs [Peters et al., 1987; Martinez-Peralta et al., 1990]. We document the rapidly fatal consequences of intravenous LCMV-WE inoculation compared with the absence of disease after inoculation via intragastric gavage, and we note critical differences between the outcomes for guinea pigs, nonhuman primates, and humans.

MATERIALS AND METHODS

Virus Stocks

LCMV-WE was originally isolated from a patient whose initials are recorded as WE [Rivers and Scott, 1935, 1936], although some investigators have reported WE to mean “Western strain” [Montali et al., 1995] or the initials of the Walter and Eliza Hall in Australia. The LCMV-WE stock was obtained from David Bishop, who received his stock from Fritz Lehmann-Grube, and the viral sequence has been published [Romanowski et al., 1985; Djavani et al., 1998]. The stock was passaged through Vero cells at Fort Detrick, Maryland, where it was established that 10^4 plaque-forming units (pfu) delivered subcutaneously is a lethal dose (by day 13/14) in cynomolgus macaques. The stock was amplified in Vero cells and stored at 10^7 pfu/ml. LCMV-Armstrong 53b strain, used to inoculate one of the monkeys, has been described previously [Salvato et al., 1988, 1989; Salvato and Shimomaye, 1989]. Both strains, LCMV-Armstrong and LCMV-WE, replicate to similar levels in mice when inoculated intragastrically [Rai et al., 1996, 1997] (also M.S. Salvato, unpublished observations).

Rhesus Monkeys and Inoculations

All experimental procedures and protocols were reviewed and approved by the Institutional Animal Care and Use Committee. Methods were consistent with the Panel on Euthanasia of the American Veterinary Medical Association. Necropsy was conducted in a negative-pressure, Hepa-filtered room and protective gear included respirators (Hepa 12 Air-supply units; Lab Safety Supply #0E-67642, Janesville, WI) and barrier clothing (e.g., disposable Tyvek jump suits, boots, gloves, and face shields; Fisher Scientific, Pittsburgh, PA).

Rhesus monkeys in excellent health were acclimatized for a week in the BSL-2/3 facility. They were all 2–5-year-old females with normal weights and activity levels. One monkey (Rh-ig6c) was euthanized 72 hr after intragastric (i.g.) inoculation with 10^6 pfu LCMV-Armstrong, so that virus distribution could be observed immediately after inoculation. Two additional monkeys, Rh-iv3 and Rh-iv6, were used for i.v. inoculation with 10^3 pfu and 10^6 pfu, respectively, and two, Rh-ig6a and Rh-ig6b, were used for i.g. inoculation with 10^6 pfu LCMV-WE. The animals to be inoculated by the intragastric route were first anesthetized (ketamine, 20 mg/kg) and given 1 ml of virus in phosphate-buffered saline (PBS) by gavage; the animals

inoculated intravenously were anesthetized and given 0.5 ml of virus in PBS via the left calf vein. Animals were observed daily and temperatures were taken by rectal or skin-patch thermometer (Traxit, Medical Indicators, Carlsbad, CA).

Blood Analyses for Chemistry, Hematology, and Lymphocyte Subsets

Blood samples were drawn at weekly intervals from the saphenous vein and submitted to the clinical laboratory for complete blood counts and standard 20 assay chemistry panels as described [Hinds et al., 1997]. Peripheral blood mononuclear cells (PBMC) were obtained from anticoagulant-treated blood centrifuged over Ficoll-Hypaque as described by Pauza et al. [1997], and flow cytometry was used to determine changes in white blood cell subsets. After paraformaldehyde fixation and antibody staining, $CD4^+$, $CD8^+$, and $CD20^+$ lymphocyte subsets were identified using FITC-conjugated monoclonal antibody against CD4 or CD8 (Antigenix America, Franklin Square, NY), or FITC-conjugated anti-CD20 (Becton Dickinson, Mountain View, CA), using relevant isotype controls as described [Pauza et al., 1997]. Samples were analyzed on a FACScan flow cytometer (Becton-Dickinson), and data were processed using Becton Dickinson Cell Quest software. Absolute counts were determined by multiplying the percentage for each subset by the absolute lymphocyte count obtained from clinical hematology data. Sera were analyzed by enzyme-linked immunosorbent assay (ELISA) for LCMV antibodies as described [Rai et al., 1996].

Detection of Infectious Virus in Tissue Samples

Whole cells from spleen and lymph nodes were used for infectious center assays. Spleens and lymph nodes were obtained at necropsy and placed in RPMI + 10% fetal calf serum (FCS) on ice for immediate processing. Tissue pieces were passed through wire mesh and the suspended monocytes were collected, washed, and counted. They were plated in 6-well plates on sparse Vero cell monolayers. The number of plaques visible by crystal violet staining are described per 10^3 cells. Plasma collected weekly and ground tissues obtained after necropsy were assayed for LCMV plaques on Vero cell monolayers as previously described [Doyle and Oldstone, 1987].

Immunohistochemistry to Detect Viral Antigen in Tissues

Immunohistochemistry was performed according to the manufacturer's recommendations for the Cell and Tissue Staining kit (R & D Systems, Minneapolis MN). Briefly, formalin-fixed, paraffin-embedded tissue sections were deparaffinized, unmasked with heat, blocked with normal human serum and incubated with hyper-immune guinea pig serum 1:50 overnight at room temperature. Sections were washed in PBS and incubated for 1 hr at room temperature with biotin-labeled goat anti-guinea pig serum (Sigma Chemical Co., St. Louis. MO).

In Situ Hybridization to Detect Viral RNA

In situ hybridization was performed as described [Hirsch et al., 1995; Yin et al., 1998] with digoxigenin-labeled RNA probes generated by SP6 or T7 polymerase transcription from the entire LCMV GP gene. Briefly, formalin-fixed, paraffin-embedded tissue sections were hybridized with 1.50 ng/ml of the riboprobes at 52°C overnight, washed in 2× SSC/50% formamide solution, 2× SSC and treated in an RNase solution for 30 min at 37°C (RNase T1 and RNase A). The slides were blocked with a buffer containing 2% horse serum, 150 mM NaCl and 100 mM Tris, pH 7.4, for 1 hr. After nonspecific blocking, the slides were incubated for 1 hr with sheep anti-digoxigenin alkaline phosphatase conjugate (Boehringer-Mannheim, Indianapolis, IN) at 1:500 dilution, rinsed in Tris, pH 7.4, and incubated overnight at room temperature with NBT/BCIP (Vector, Burlingame, CA) substrate in the dark. The stained slides were rinsed in water, counterstained with nuclear fast red, dehydrated, and covered with glass

coverslips. Controls included LCMV GP sense probe hybridized on LCMV-infected tissues and anti-sense LCMV-GP probe on uninfected tissues.

RT-PCR to Detect Viral RNA

Primers for LCMV-WE glycoprotein (GP) and nucleocapsid protein (NP) have been described [Stephensen et al., 1992]: GP (1–19) CGCACCGGGGATCCTAGGC is the forward primer and GP (499–480) ATACTCATGAGTGTATGGTC is the reverse primer. NP primers covered nucleotides 3375–3357, CGCACAGTGGATCCTAGGC and nucleotides 3172–3194, GCTGACTTCAGAAAAGTCCAACC. RNA extracted from monkey tissues was converted to cDNA using these specific primers and analyzed using real-time PCR as described previously [Lukashevich et al., 1999]. Levels of viral RNA were evaluated using SYBR Green technology, and amplification plots were expressed as C_T values to be analyzed with 5700 Sequence Detection System (SDS) software (Perkin-Elmer Systems). The C_T is the reaction cycle at which the PCR products, or amplicons, reach a threshold level of detection: the lower the C_T value the more abundant the substrate. C_T values were normalized by using glyceraldehyde 3-phosphate dehydrogenase (GAPDH) amplicons as an internal standard. Dissociation analysis of the PCR products was used to confirm specificity.

To detect LCMV-Armstrong RNA in the animal that was euthanized at 72 hr, primers were used according to sequence accession no. M20869 generating a 246-bp fragment: ArmGP-F118 (TCATCGATGAGGTGATCAAC) and ArmGp-R364 (TTGTTGGCTGAACATGCGTTG). Comparable LCMV-WE-specific primers were generated (WEGpF55, GCTGGATTCTATCCAGTAA, and WEGpR342, GCATCGTCAGATTTAAGTGA) to ensure that none of the LCMV-Armstrong-infected samples exhibited cross-contamination with LCMV-WE and vice versa.

RESULTS

Clinical Observations Revealed Little Disturbance of i.g.-Inoculated Monkeys and Severe Morbidity in i.v.-Inoculated Monkeys

Except for the monkey euthanized at 72 hr, all the monkeys appeared healthy for the first 4 days after virus inoculation. On day 5, three of four monkeys experienced a slight rise in body temperature (Table I), and their pelage appeared greasy and unkempt. By day 7, all had slightly elevated body temperatures and appeared ungroomed. By day 8, the two i.v.-inoculated animals developed slight temperatures (103–104°F), while the two i.g.-inoculated animals appeared normal (101°F) and remained healthy until their necropsy 3 weeks later. By day 9, the two i.v.-inoculated animals had fever (105°F), had stopped eating, and had become anorectic; they were found crouching and shivering in their cages. Aspirin was given as a palliative at 20 mg/kg three times daily. Because of diarrhea, orbital hemorrhage, and hypovolemic shock, animals were euthanized with an overdose of pentobarbital on day 11.

Changes were observed in blood chemistry and hematology in i.v.-inoculated monkeys but not in the i.g.-inoculated monkeys. All animals were seronegative.

Blood was sampled on days 14 and 7 before virus inoculation, on the day of inoculation, on day 7 after inoculation and weekly until necropsy. Absolute counts of white blood cell subsets ($CD4^+$, $CD8^+$, and $CD20^+$ cells) were determined by a combination of hematology and flow cytometry, as described in Materials and Methods, and all lymphocyte subsets maintained baseline values of 500–2,000 cells/ml. There were only two notable deviations from the baseline values: (1) Rh-iv3 spiked to 3,300 $CD8^+$ cells/ml on the day of necropsy (day 11), and (2) Rh-ig6a spiked to 5,000 $CD8^+$ cells/ml on day 15. Hematological analyses are shown

in Table II and blood chemistries in Table III with those values underlined that lie outside the normal range for rhesus macaques.

Abnormally high levels of both alanine aminotransferase (ALT) and aspartate aminotransferase (AST) liver enzymes were observed in the i.v.-inoculated monkeys. These enzymes were elevated at day 7 post infection and increased by 3- and 7-fold for rh-iv3 and rh-iv6, respectively, by the day of death, indicating that liver dysfunction is an early sign of infection. At day 11 the level of GGT (γ-glutamyltransferase), a very sensitive test for liver damage, was also elevated in the i.v.-inoculated animals (Table III). Increased iron, alkaline phosphatase (AP) and total bilirubin (for rh-iv6) indicated that a cholestatic component (poor bile circulation) was involved and could also contribute to poor liver function.

All monkeys were seronegative for LCMV before infection, during infection, and upon necropsy. The i.v.-inoculated animals died before an immune response had a chance to reach detectable levels, and the i.g.-inoculated animals had insufficient antigenemia to drive a detectable serological response.

Necropsy Showed Hemorrhagic Disease in i.v.-Inoculated Monkeys and No Significant Disease in i.g.-Inoculated Monkeys

By 11 days after inoculation, Rh-iv6 and Rh-iv3 displayed signs of severe dehydration, fever, and distress (matted, ungroomed hair), and were euthanized on day 11. As per standard procedure, they were administered 15 mg/kg ketamine, intramuscular, followed by sodium pentobarbital given i.v. at 50 mg/kg. None of the monkeys inoculated by gavage displayed overt disease signs. Rh-ig6c was sacrificed at 72 hr after inoculation for an analysis of virus tissue distribution. Rh-ig6a and Rh-ig6b were sacrificed 28 days after inoculation.

Macroscopic Pathological Findings

On gross postmortem examination, animal Rh-iv6 weighed 3.5 kg and was judged to be in thin nutritional condition (Table IV). Dehydration was severe (10–12%), and the periorbital skin was erythematous. In the subcutis over the right parietal region of the head a 1-cm-diameter, round area of hemorrhage was present. The inguinal and axillary lymph nodes were moderately enlarged. The lungs were mottled light and dark red and could be infused with formalin only under moderate pressure. The small intestine for Rh-iv6 had diffuse transmural reddening, with the tinctural intensity increasing in the distal segments. The mucosal surface of the bladder had mild, scattered petechia. The femoral bone marrow was scant and dark red-yellow.

Upon necropsy, Rh-iv3 was 3 kg and in thin nutritional condition. Two digits of the left hand had small bleeding foci over the phalanges. Gross pathology for Rh-iv3 was similar to that described for Rh-iv6 pertaining to the general condition, lungs, bone marrow, and bladder (Table IV). The condition of the lungs was less severe for Rh-iv3 than for Rh-iv6. Rh-iv3 had moderate hemorrhage around all venipuncture sites, and moderate petechia present on the mucosal surface of the stomach. Unlike Rh-iv6, no increase in size was noted in the peripheral lymph nodes. In contrast to the two i.v.-inoculated monkeys, no significant lesions were present on gross postmortem examination of Rh-ig6a, and Rh-ig6b.

Microscopic Pathological Findings

Histopathology on Rh-iv6 demonstrated moderate pulmonary edema, characterized by multifocal to regionally extensive filling of alveoli with homogeneous to granular eosinophilic material accompanied by small numbers of macrophages (Figs. 1–2). Sections of lungs from both Rh-iv6 and Rh-iv3 had moderate multifocal perivascular edema and hemorrhage. The histopathology of Rh-iv3 was comparable to Rh-iv6, only less severe (Table IV). Both i.v.-inoculated animals also had necrotic foci on the buccal cavity. Both had severe, diffuse

depletion of bone marrow cells, with infiltration of adipocytes. Myeloid to erythroid ratios (M:E) were 1:2 for Rh-iv6 and 1:1 for Rh-iv3. Other significant findings in both monkeys included severe diffuse depletion of thymic lobules, with only scant numbers of small lymphocytes surrounding Hassall's corpuscles, and mild to moderate, randomly scattered hepatocellular necrosis (Figs. 1 and 2). Only minimal mixed inflammatory cells (macrophages and lymphocytes) were present adjacent to the necrotic hepatocytes. Both animals had sinus histiocytosis of inguinal and axillary lymph nodes, but Rh-iv6 had paracortical lymphoid hyperplasia; Rh-iv3 had moderate generalized follicular depletion. Rh-iv3 also had mild to moderated mucosal hemorrhage of both the stomach and bladder, with submucosal edema of the latter.

Minor histopathology was noted in tissues examined from the i.g.-inoculated monkeys Rh-ig6a and Rh-ig6b (Table V). Both monkeys had gastritis and activated spleen and lymphoid tissues, but these could have been incidental to their inoculation with virus, as they are often observed in uninfected monkeys.

Detection of Virus in Tissue Samples

Cells obtained from spleen and lymph nodes of i.v.-inoculated monkeys were positive for LCMV by infectious center assay, but cells from the i.g.-inoculated monkeys were not (Table VI). Likewise, plasma and tissue samples from the i.v.-inoculated monkeys were positive for LCMV by plaque assay on Vero cell monolayers, but samples from the i.g.-inoculated monkeys were not (Table VI).

In situ hybridization of monkey tissues revealed abundant viral nucleic acids in the liver and lymph nodes of the i.v.-inoculated animals, but only background hybridization in the i.g.-inoculated animals (Fig. 3). Immunohistochemistry of monkey tissues (spleen, liver, kidney, thymus, lung, bone marrow, hippocampus, and mesenteric lymph nodes) revealed scattered foci of infection in all organs for the i.v.-inoculated animals but none for the i.g.-inoculated animals. Immunohistochemistry of liver, the organ with highest titer, is depicted in Figure 4.

RT-PCR Demonstrated Infection of Both i.v.- and i.g.-Inoculated Monkeys

Virus-specific nucleic acids were detected by reverse transcription followed by PCR of RNA extracted from monkey plasma or tissues (Table VII). Monkeys Rh-iv3, Rh-iv6, Rh-ig6a, and Rh-ig6b were all inoculated with LCMV-WE. WE-specific nucleic acid could only be detected when WE-specific oligonucleotide primers were used, and could not be detected when LCMV-Armstrong-specific primers were used. Monkey Rh-ig6c was inoculated with LCMV-Armstrong, and nucleic acid could only be detected when Armstrong-specific primers were used, and not when LCMV-WE primers were used (Fig. 5, Table VII). Viral nucleic acid was strongly detected in the i.v.-infected monkeys by day 7 after inoculation (i.e. Table VII shows a low C_T, < 36 for viral amplicons in comparison to background $C_T = 40$). By contrast, nucleic acid was only faintly detected in the plasma of Rh-ig6a and Rh-ig6b two to three weeks after inoculation (faint detection means a $C_T > 36$ or very close to the background level of 40) (Table VII). By the fourth week, there was no detectable viral RNA in the plasma of the i.g.-inoculated monkeys. Monkey Rh-ig6c was euthanized 72 hr after inoculation and LCMV-Armstrong-specific nucleic acid could be detected in PBMC, spleen, stomach (Fig. 5), and most tissues assessed (data not shown). Tissue samples from Rh-ig6c were negative for LCMV-WE and for Pichinde RNA (both arenaviruses commonly used in this laboratory), thus there was no contamination from those viruses during sample processing.

DISCUSSION

The route of arenavirus infection is critical to clinical outcome [Fisher-Hoch, 1993]. We inoculated five rhesus macaques with LCMV to compare intravenous and intragastric routes of infection. The two macaques given intravenous virus became moribund quickly, exhibiting hypovolemic shock secondary to a widely disseminated hemorrhagic infection. The animals given virus by gavage had attenuated transient infections which did not lead to disease.

Evidence for infection in the gavaged animals is solely by detection of viral nucleic acids in PBMC and tissues. In the monkey euthanized at 72 hr, viral nucleic acid was detected in most tissues examined. Virus nucleic acid was detectable in plasma of the other two i.g.-inoculated monkeys at week 3, but not at weeks 1, 2, or 4. For all the i.g.-inoculated animals, virus was never detected in any tissue by plaque assay, nor was viral nucleic acid detected by in situ hybridization. In contrast, virus was readily detected in the i.v.-inoculated animals by plaque assay, and virus nucleic acid was detected by in situ hybridization, and by RT-PCR. The i.g. animals were only inoculated with 10^6 pfu of infectious virus, and this amount of virus would not be detectable after tissue dissemination in the absence of virus replication. Thus, the viral nucleic acid found in tissues constitutes evidence for an attenuated, transient infection. The detected viral nucleic acids are most likely the result of infection and not the result of laboratory contamination because strain-specific primers were used for PCR and no cross-detection occurred; i.e., the animal infected with LCMV-Armstrong could only be detected by Armstrong-specific primers and the animals infected with LCMV-WE could only be detected with WE-specific primers. Despite 16% nucleotide sequence divergence [Romanowski et al., 1985; Salvato et al., 1988; Djavani et al., 1998], LCMV-WE and LCMV-Armstrong strains showed no difference in ability to infect mice after intragastric inoculation, and are known to establish disseminated infection in mice after only 72 hr [Rai et al., 1997].

Subclinical transient mucosal infection of rhesus macaques by simian immunodeficiency virus (SIV) has been well documented in the rhesus/acquired immunodeficiency syndrome (AIDS) model [Pauza et al., 1993]. Animals that had been intrarectally inoculated with low doses of SIV were never seropositive or viremic. Viral nucleic acids were also not detectable by PCR at 2 months after inoculation, but could be detected by PCR three months after inoculation [Pauza et al., 1993]. Blood transfused from an aviremic monkey was capable of initiating full-blown infection in a naive animal, showing that the mucosal route gave the animal a chance to develop immune responses that attenuated the infection by the time virus was broadly circulated in the blood [Pauza et al., 1993]. The LCMV model described is similar to the rhesus/AIDS model in that the virus is only detectable by amplification of viral nucleic acids from tissues and causes no overt disease.

Although arenaviruses readily establish persistent subclinical infections in carrier rodents, subclinical infections, persistent or otherwise have not been studied in primates. LCMV infection leading to fetal defects like hydrocephalus and chorioretinitis has been documented in human beings [Barton and Mets, 2001] in which two-thirds of fetal LCMV cases can be traced to an acute maternal illness. Thus, it is unknown whether a subclinical infection, such as that seen in our gavaged animal model could contribute to such an outcome. We speculate that subclinical infection of the mother would not lead to fetal defects since the fetus probably shares the innate mechanisms that make the mucosal infection self-limiting.

Disease in the i.v.-inoculated monkeys was similar to published descriptions of human and nonhuman primates with arenaviral hemorrhagic fevers [Peters, 1997; Fisher-Hoch, 1993]. Histopathology of the lungs resembled the description of rhesus macaques infected with LCMV-WE by aerosol: interstitial pneumonia with edema, histiocytic infiltrates, and hemorrhage [Danes et al., 1963]. In both rhesus and cynomolgus macaque species, morbidity

was observed within 13 days and virus spread from lung to mediastinal and axillary nodes to spleen, liver, kidney, and then to other organs [Danes et al., 1963]. CNS changes in infected rhesus monkeys were rarely seen, whereas cynomolgus monkeys experienced cerebral perivascular infiltrates, men-ingioencephalitis, and thickened walls of subarachnoid spaces [Danes et al., 1963]. Accordingly, in our study with rhesus macaques, we observed no significant lesions in brain sections, except for a small hemorrhage in the parietal lobe of Rh-iv6.

In our i.v.-infected animals, we noted severe lymphocyte depletion in nodes, spleen, and bone marrow. Similar depletion has been noted for Lassa fever [Fisher-Hoch, 1993], Argentine hemorrhagic fever of rhesus macaques [McKee et al., 1985], and guinea pigs [Gonzalez et al., 1987]. Such depletion could explain the impaired lymphocyte function described for Lassa infection of macaques [Fisher-Hoch et al., 1987]. A slight drop in circulating polymorphonuclear neutrophils (PMN) was observed in the two i.v.-inoculated monkeys, which is remarkable in the absence of PMN inflammatory infiltrates in lung, spleen, and liver. It would be worthwhile to investigate whether PMN are being destroyed by the infection. We also observed a dramatic drop in platelet numbers in the two i.v.-inoculated monkeys. It is notable that this thrombocytopenia is more severe in the rhesus LCMV-WE infection than in rhesus infections with Lassa virus [Fisher-Hoch et al., 1988] (also P. Jahrling, unpublished observations). It is unclear whether the thrombocytopenia is due to lack of bone marrow production, increased megakaryocyte/platelet destruction, or increased sequestration in tissues.

Liver morphology in the i.v.-inoculated monkeys was similar to that described for Lassa: a mild multifocal necrosis without significant inflammatory response, hence inadequate to account for death due to hepatic failure [Fisher-Hoch, 1993]. Acute lesions in Lassa virus infections are also minimal and without significant inflammatory infiltrations [Fisher-Hoch, 1993]. Nevertheless, there is slightly more hepatic damage in the LCMV-WE-infected monkeys than normally seen in Lassa fever (I. Lukashevich, personal observation). Also, there is greater discrepancy between AST and ALT in Lassa [McCormick et al., 1986] than in LCMV WE disease (herein), indicating that Lassa includes significant extrahepatic damage. The absence of inflammation observed in human/primate infections with Lassa and LCMV-WE contrasts with the extensive PMN infiltrates observed in LCMV-WE-infected guinea pigs [Martinez-Peralta et al., 1990]. In the guinea pig model, PMN are initially essential for antiviral defense; however, late in infection, PMN cause massive tissue destruction, primarily in spleen and lung [Gonzalez et al., 1987]. Morbidity in the rhesus model described, as well as death in Lassa fever, Argentine hemorrhagic fever, and Bolivian hemorrhagic fever is due to vascular dysfunction and subsequent circulatory failure [Ruggiero et al., 1964; Fisher-Hoch, 1993].

Hypovolemic shock and hemorrhage result either from directly damaged vasculature or to inadequate repair of damaged vasculature. Unlike the filoviruses, Marburg and Ebola, that destroy vascular endothelial cells in culture [Schnittler et al., 1993; Feldmann et al., 1996; Yang et al., 1998; Baize et al., 1999], arenaviruses like Lassa fever virus do not destroy cultured endothelial cells, but do diminish their capacity to express chemokines [Fisher-Hoch et al., 1987; Schnittler et al., 1993; Lukashevich et al., 1999]. Also unlike Ebola and Marburg hemorrhagic disease, Lassa fever disease does not cause an increase in fibrinogen breakdown products or diffuse intravascular coagulation (DIC) [Fisher-Hoch et al., 1988]. With Lassa, there is a defect in platelet aggregation that corresponds to severity of disease [Cummins et al., 1989a,b]; however, platelet and fibrinogen turnover rates are normal in experimental primate infections [Fisher-Hoch et al., 1987]. Thus, the bleeding disorder in Lassa-infected animals has been attributed to an unknown soluble factor affecting platelet function and arresting megakaryocyte maturation [Roberts et al., 1989]. Our observation of LCMV-infected rhesus macaques reveals a drop in platelets from 400–500/μl to 40–90/μl that directly explains decreased coagulation and inadequate vascular repair. Thus, the vascular damage observed in

the i.v.-infected monkeys is more likely due to defects in vascular repair than to viral destruction of vascular endothelial cells.

Outcomes in arenavirus fevers are associated with virus dose and level of replication, i.e. serum titers above 10^3 $TCID_{50}$/ml are generally associated with severe disease [McCormick et al., 1987]. As expected, Rh-iv6 achieved higher serum titers than Rh-iv3 and showed more severe disease signs. Infection across the gastric mucosa could effectively reduce viral dose, and hence pathogenesis, by acting as a natural barrier to high viral doses. It may also be that the mucosal barrier is contributing to local immune responses that attenuate and eventually eliminate LCMV infection. Most commonly in mucosal viral infections, virus gets to the periphery but fails to cause disease because it has been attenuated, either by selection of attenuated variants or by eliciting a protective immune response [Pauza et al., 1993]. As suggested by murine experiments, ingestion of arenavirus [Rai et al., 1997] and of vectors expressing viral antigens [Djavani et al., 2000, 2001] provides immunity to lethal disease. Circumstantial evidence for mucosal immunity through virus ingestion comes from field observations: many individuals living in close contact with rodents and ingesting rodent-contaminated food are seropositive for Lassa virus but have never experienced Lassa fever disease [ter Meulen et al., 1996; Lukashevich et al., 1993; Childs and Peters, 1993]. Whether the mucosa simply serves to reduce the inoculum, to select attenuated variants, or to provide a protective immune response, it is clear that the mucosal route attenuates the infection substantially in comparison to the intravenous route.

Acknowledgements

The authors are grateful to Joan Geisbert for sending the LCMV-WE stock from Ft. Detrick, to Leonard Acker for animal care, to Joan Scheffler for establishing the rhesus normal value ranges (Tables II and III), and to C. David Pauza for reading this manuscript. We are also grateful to Drs. Miroslav Malkovsky and Mikulas Popovic for translations (Czechoslovakian to English) of the article by Danes et al. [1963]. The work was supported by NIH grant RO1-RR13980 (to I.S.L.).

Grant sponsor: National Institutes of Health; Grant number: RO1-RR13980.

References

Armstrong C, Lillie RD. Experimental lymphocytic choriomeningitis of monkeys and mice produced by a virus encountered in studies of the 1933 St. Louis encephalitis epidemic. Public Health Rep (Wash) 1934;49:1019–1027.

Baize S, Leroy EM, Courbot-Georges M-C, Capron M, Soukate-Lansoud J, Debre P, Fisher-Hoch S, McCormick J, Georges AJ. Defective humoral responses and extensive intravascular apoptosis are associated with fatal outcome in Ebola virus-infected patients. Nature Med 1999;5:423–426. [PubMed: 10202932]

Barton LL, Mets MB. Congenital lymphocytic choriomeningitis virus infection: decade of rediscovery. Clin Infect Dis 2001;33:370–374. [PubMed: 11438904]

Childs, JE.; Peters, CJ. Ecology and epidemiology of arenaviruses and their hosts. In: Salvato, MS., editor. The Arenaviridae. New York: Plenum Press; 1993. p. 331-384.

Cummins D, Bennett D, Fisher-Hoch SP, Farrar B, McCormick JB. Electrocardiographic abnormalities in patients with Lassa fever. J Trop Med Hyg 1989a;92:350–355. [PubMed: 2810453]

Cummins D, Fisher-Hoch SP, Walshe KJ, Mackie IJ, McCormick JB, Bennett D, Perez G, Farrar B, Machin SJ. A plasma inhibitor of platelet aggregation in patients with Lassa fever. Br J Haematol 1989b;72:543–548. [PubMed: 2775659]

Danes L, Benda R, Fuchsova M. Experimentalni inhalacni nakaza opic druhu macacus cynomolgus a macacus rhesus virem lymphocitarni choriomeningitidy (kmenem WE) [in Czechoslovakian]. Bratisl Lek Listy 1963;43:71–79. [PubMed: 14065052]

Djavani M, Lukashevich IS, Salvato MS. Sequence comparison of the large genomic RNA segments of two strains of lymphocytic choriomeningitis virus differing in pathogenic potential for guinea pigs. Virus Genes 1998;12:149–153.

Djavani M, Cheng Y, Xia L, Lukashevich IS, Pauza CD, Salvato MS. Murine immune responses to mucosally delivered *Salmonella* expressing Lassa fever virus nucleoprotein. Vaccine 2000;18:1543–1554. [PubMed: 10618553]

Djavani M, Yin C, Lukashevich IS, Rodas J, Rai SK, Salvato MS. Mucosal immunization with *S. typhimurium* expressing Lassa virus NP cross-protects mice from lethal challenge with LCMV. J Hum Virol 2001;4:103–108. [PubMed: 11437313]

Doyle MV, Oldstone MBA. Interactions between viruses and lymphocytes. I. In vivo replication of lymphocytic choriomeningitis virus in mononuclear cells during both chronic and acute viral infections. J Immunol 1987;121:1262–1269. [PubMed: 308960]

Feldmann H, Bugani H, Mahner F, Klenk HD, Drenckhahn D, Schnittler HJ. Filovirus-induced endothelial leakage triggered by infected monocytes/macrophages. J Virol 1996;70:2208–2214. [PubMed: 8642644]

Fisher-Hoch, SP. Arenavirus pathophysiology. In: Salvato, MS., editor. The arenaviruses. New York: Plenum Press; 1993. p. 299-323.

Fisher-Hoch SP, Mitchell SW, Sasso DR, Lange JV, Ramsey R, McCormick JB. Physiologic and immunologic disturbances associated with shock in Lassa fever in a primate model. J Infect Dis 1987;155:465–472. [PubMed: 3543155]

Fisher-Hoch SP, McCormick JB, Sasso D, Craven RB. Hematologic dysfunction in Lassa fever. J Med Virol 1988;26:127–135. [PubMed: 3183637]

Gonzalez PH, Ponzinibbio C, Laguens RP. Effect of polymorphonuclear depletion on experimental Argentine hemorrhagic fever in guinea pigs. J Med Virol 1987;22:289–294. [PubMed: 3040897]

Hinds PW, Yin C, Salvato MS, Pauza CD. Pertussis toxin-induced leukocytosis in rhesus macaques. J Med Primatol 1997;25:1–7.

Hirsch VM, Dapolito G, Johnson PR, Elkins WR, London WT, Montali RJ, Goldstein S, Brown C. Induction of AIDS by simian immunodeficiency virus from an African green monkey: species-specific variation in pathogenicity correlates with the extent of in vivo replication. J Virol 1995;69:955–962. [PubMed: 7815563]

Lukashevich IS, Clegg JCS, Sidibe K. Lassa virus activity in Guinea: distribution of human antiviral antibody defined using enzyme-linked immunosorbent assay with recombinant antigen. J Med Virol 1993;40:210–217. [PubMed: 8355019]

Lukashevich IS, Maryankova R, Vladyko AS, Nashkevich N, Koleda S, Djavani M, Horejsh D, Voitenok NN, Salvato MS. Lassa and Mopeia virus replication in human monocytes/macrophages and in endothelial cells: different effects on IL-8 and TNF-α gene expression. J Med Virol 1999;59:552–560. [PubMed: 10534741]

Martinez-Peralta LA, Laguens M, Ponzinibbio C, Laguens RP. Infection of guinea pigs with two strains of lymphocytic choriomeningitis virus. Medicina (Buenos Aires) 1990;50:225–229.

McCormick, J. Arenaviruses. In: Fields, BN.; Knipe, DM.; Howley, PM., editors. Field's virology. 2. 1. New York: Lippincott-Raven Press; 1990. p. 1245-1267.

McCormick JB, Walker DH, King IJ, Webb PA, Elliott LH, Whitfield SG, Johnson KM. Lassa virus hepatitis: a study of fatal Lassa fever in humans. Am J Trop Med Hyg 1986;35:401–407. [PubMed: 3953952]

McCormick JB, Webb PA, Krebs JW, Johnson KM, Smith ES. A prospective study of the epidemiology and ecology of Lassa fever. J Infect Dis 1987;155:437–442. [PubMed: 3805771]

McKee KT, Mahlandt BG, Maiztegui JE, Eddy GA, Peters CJ. Experimental Argentine hemorrhagic fever in rhesus macaques: virus strain-dependent clinical response. J Infect Dis 1985;152:218–221. [PubMed: 2989384]

Montali RJ, Scanga CA, Pernikoff D, Wessner DR, Ward R, Holmes KV. A common source outbreak of callitrichid hepatitis in captive tamarins and marmosets. J Infect Dis 1993;167:946–950. [PubMed: 8450260]

Montali RJ, Connolly BM, Armstrong DL, Scanga CA, Holmes KV. Pathology and immunohistochemistry of callitrichid hepatitis, an emerging disease of captive New World primates caused by lymphocytic choriomeningitis virus. Am J Pathol 1995;147:1441–1449. [PubMed: 7485406]

Pauza CD, Emau P, Salvato MS, Trivedi P, MacKenzie D, Malkovsky M, Uno H, Schultz KT. Pathogenesis of SIVmac251 after atraumatic inoculation of the rectal mucosa in rhesus monkeys. J Med Primatol 1993;22:154–161. [PubMed: 8411107]

Pauza CD, Hinds PW II, Yin C, McKechnie TS, Hinds SB, Salvato MS. The lymphocytosis promoting agent pertussis toxin affects virus burden and lymphocyte distribution in the SIV-infected rhesus macaque. AIDS Res Hum Retroviruses 1997;13:87–95. [PubMed: 8989431]

Peters, CJ. Viral hemorrhagic fevers. In: Nathanson, N., editor. Viral pathogenesis. New York: Lippincott-Raven; 1997. p. 779-799.

Peters CJ, Jahrling PB, Liu CT, Kenyon RH, McKee KT, Barrera Oro JG. Experimental studies of arenaviral hemorrhagic fevers. Curr Top Microbiol Immunol 1987;134:5–68. [PubMed: 3034512]

Rai SK, Wu M, Cheung D, Warner T, Salvato MS. Murine infection with lymphocytic choriomeningitis virus following gastric inoculation. J Virol 1996;70:7213–7218. [PubMed: 8794369]

Rai SK, Micales BK, Wu MS, Cheung DS, Pugh TD, Lyons GE, Salvato MS. Timed appearance of lymphocytic choriomeningitis virus after gastric inoculation of mice. Am J Pathol 1997;151:633–639. [PubMed: 9250174]

Rivers TM, Scott TFM. Meningitis in man caused by a filterable virus. Science 1935;81:439–440. [PubMed: 17750170]

Rivers TM, Scott TFM. Meningitis in man caused by a filterable virus. II. Identification of the etiological agent. J Exp Med 1936;63:415–432.

Roberts P, Cummins D, Bainton AL, Walshe KJ, Fisher-Hoch SP, McCormick JB, Gribben JG, Machin SJ, Linch DC. Plasma from patients with severe Lassa fever profoundly modulates f-met-leu-phe induced superoxide generation in neutrophils. Br J Haematol 1989;73:152–157. [PubMed: 2554951]

Romanowski V, Matsuura Y, Bishop DHL. Complete sequence of the S RNA of lymphocytic choriomeningitis virus (WE strain) compared to that of Pichinde arenavirus. Virus Res 1985;3:101–114. [PubMed: 4060885]

Ruggiero HR, Parodi AS, Ruggiero HG, Mettler N, Boxaca M, de Guerrero AL, Cimtora A, Magnoni C, Milani H, Maglio F, Gonzales-Cambaceres C, Astarloa L, Squassi G, Fernandez D, Giacosa A. Fiebre hemorragica Argentina. I. Periodo de incubacion e invasion. Rev Assoc Med Argent 1964;78:221–226.

Salvato, MS.; Rai, SK. The arenaviruses. In: Collier, L.; Mahy, B., editors. Topley and Wilson's principles of bacteriology, virology, and immunity. London: Edward Arnold Ltd; 1996. p. 629-650.

Salvato MS, Shimomaye EM. The completed sequence of lymphocytic choriomeningitis virus reveals a unique RNA structure and a gene for a zinc finger protein. Virology 1989;173:1–10. [PubMed: 2510401]

Salvato M, Shimomaye E, Southern P, Oldstone MBA. Virus lymphocyte interactions. IV. Molecular characterization of LCMV Armstrong (CTL^+) and that of its variant (CTL^-). Virology 1988;164:517–522. [PubMed: 3259346]

Salvato MS, Shimomaye EM, Oldstone MBA. The primary structure of the lymphocytic choriomeningitis virus L gene encodes a putative RNA polymerase. Virology 1989;169:377–384. [PubMed: 2705303]

Schnittler HJ, Mahner D, Drenckhahn D, Klenk HD, Feldmann H. Replication of Marburg virus in human endothelial cells. A possible mechanism for the development of viral hemorrhagic disease. J Clin Invest 1993;19:1301–1309. [PubMed: 8473483]

Stephensen EH, Larson EW, Dominik JW. Effect of environmental factors on aerosol-induced Lassa virus infection. J Med Virol 1984;14:295–303. [PubMed: 6512508]

Stephensen CB, Blount SR, Lanford RE, Holmes KV, Montali RJ, Fleenor ME, Shaw JF. Prevalence of serum antibodies against lymphocytic choriomeningitis virus in selected populations from two U.S. cities. J Med Virol 1992;38:27–31. [PubMed: 1402829]

ter Meulen J, Lukashevich IS, Sidibe K, Inapogui A, Marx M, Dorlemann A, Yansane ML, Koulemou K, Chang-Claud J, Schmitz H. Hunting of peridomestic rodents and consumption of their meat as possible risk factors for rodent-to-human transmission of Lassa virus in the Republic of Guinea. Am J Trop Med Hyg 1996;55:661–666. [PubMed: 9025695]

Yang Z-Y, Delgado R, Xu L, Todd RF, Nabel EG, Sanchez A, Nabel G. Distinct cellular interactions of secreted and transmembrane Ebola virus glycoproteins. Science 1998;279:1034–1037. [PubMed: 9461435]

Yin C, Djavani M, Schenkel AR, Schmidt DS, Pauza CD, Salvato MS. Dissemination of LCMV from the gastric mucosa requires G protein-coupled signaling. J Virol 1998;72:8613–8619. [PubMed: 9765400]

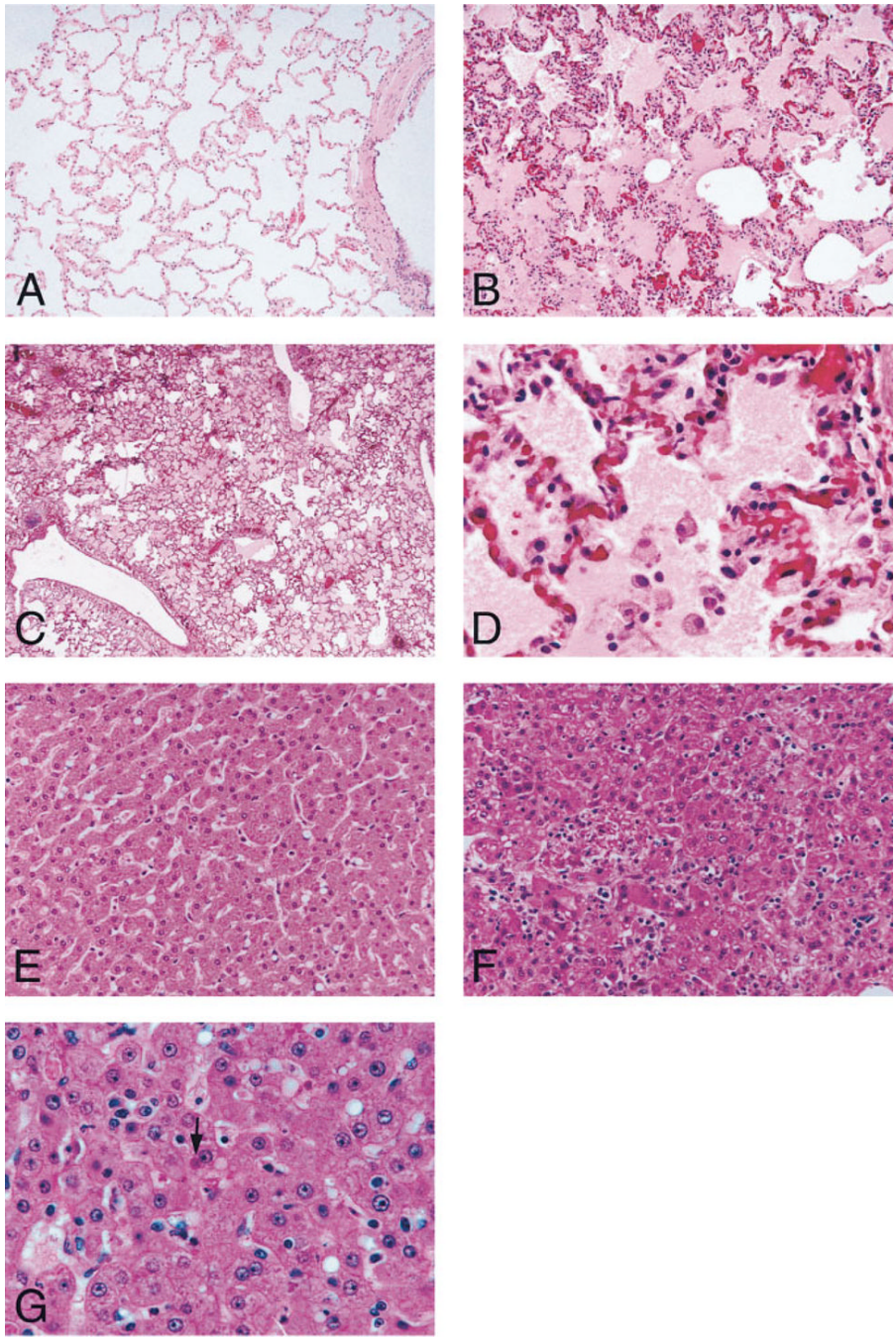

Fig. 1.

Photomicrographs of H&E-stained tissues from lymphocytic choriomeningitis virus (LCMV)-inoculated monkeys. **A:** Normal lung of a healthy animal, Rh-ig6b. **B:** Lung of Rh-iv6. Note extensive filling of alveoli with fluid, accompanied by small numbers of alveolar macrophages. **C:** Lung from Rh-iv6. **D:** Higher magnification of the lung section shown in B and C (from Rh-iv6) shows macrophage-containing fluid-filled alveoli and necrotic alveolar linings. **E:** Healthy liver from Rh-ig6b. **F:** Liver from Rh-iv3 demonstrating hepatocellular necrosis with scant inflammatory cell infiltrates. **G:** Higher magnification of liver from Rh-iv6 showing changes similar to Rh-iv3. Note the red necrotic cell at the arrow. A,B, × 100; C, ×25; D,G, × 400; E,F, × 200; G, ×40.

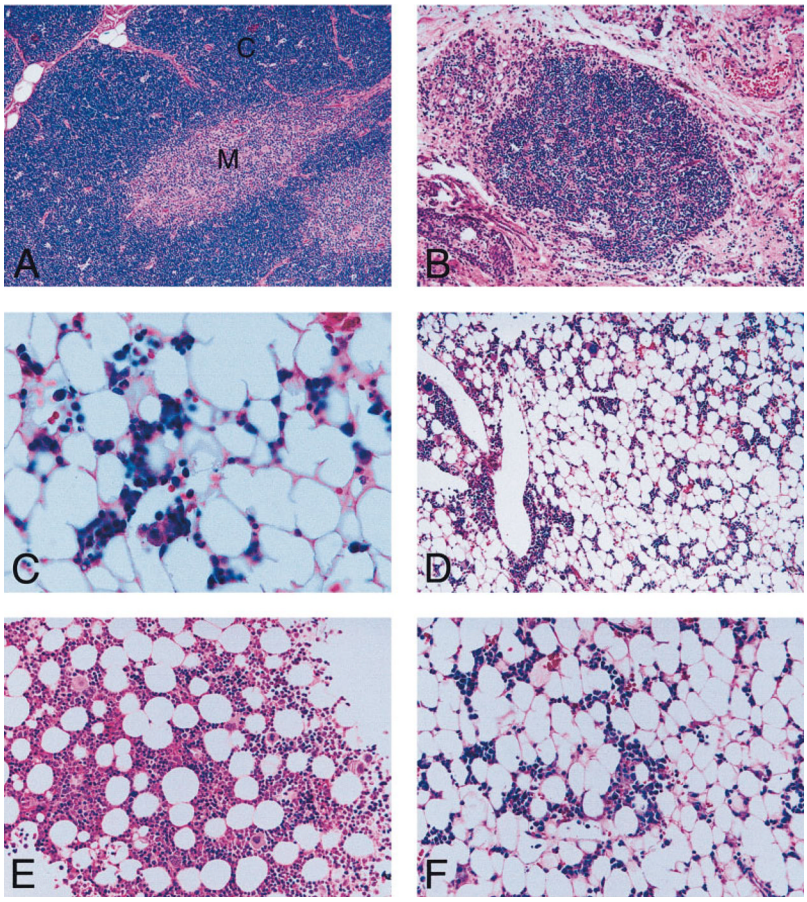

Fig. 2.

Photomicrographs of H&E-stained tissues from lymphocytic choriomeningitis virus (LCMV)-inoculated monkeys. **A:** Thymus of a healthy animal, Rh-ig6b. Cortex (C) and medulla (M) are well circumscribed. **B:** Thymus of Rh-1v6. Loss of normal structures leaves a collection of small lymphocytes surrounding the Hassall's corpuscles. **C:** Bone marrow from Rh-iv6, demonstrating decease in cellular elements and expansion of adipose tissue. **D:** Bone marrow from Rh-iv6. **E:** Bone marrow from healthy monkey, Rh-ig6a. **F:** Bone marrow from Rh-iv6. A,B,D, ×100; C, ×400; E,F, ×200.

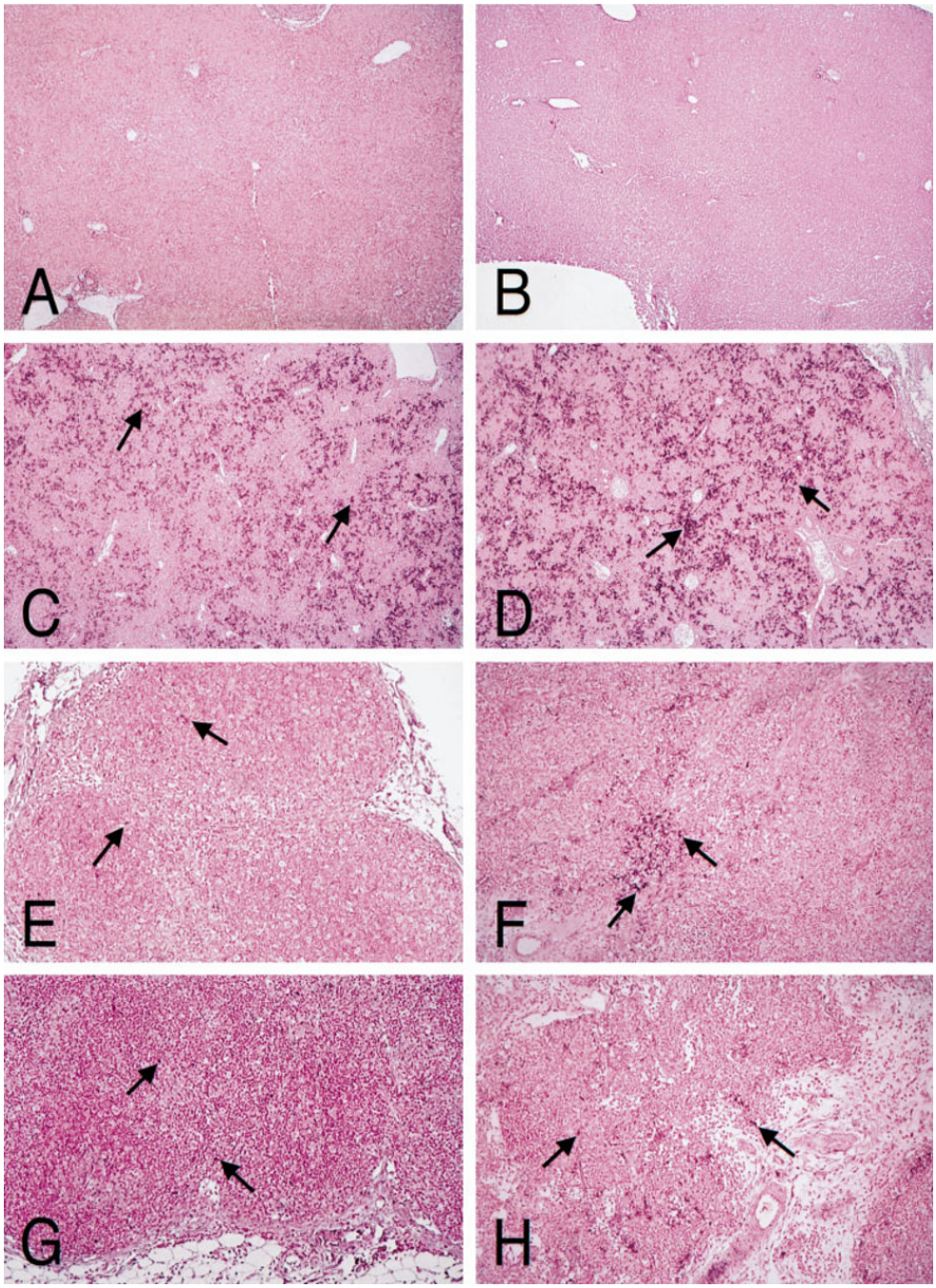

Fig. 3.

In situ hybridization of liver and lymph nodes to detect viral nucleic acid. An antisense probe to the lymphocytic choriomeningitis virus (LCMV)-WE GP gene was used to detect high concentrations of viral nucleic acid, thought to be sites of viral replication. **A,B:** Liver sections from Rh-ig6a and Rh-ig6b, respectively, showing no detectable positive hybridization sites. **C,D:** Liver sections from Rh-iv3 and Rh-iv6, respectively, showing many positive hybridization sites (dark brown spots). Lymphoid tissue sections from Rh-iv3 (**E**) and Rh-iv6 (**F**) gave these views of axillary lymph node showing scant and clustered positive hybridization sites, respectively. Mesenteric lymph node sections from Rh-iv3 (**G**) and Rh-iv6 (**H**) show dispersed hybridization sites. There were no positive signals from the i.g.-inoculated animals,

or from sections probed with the sense probe (which would detect viral replicative forms, but not viral mRNA). A,B, 25×; C,D, ×25; E–H, ×100.

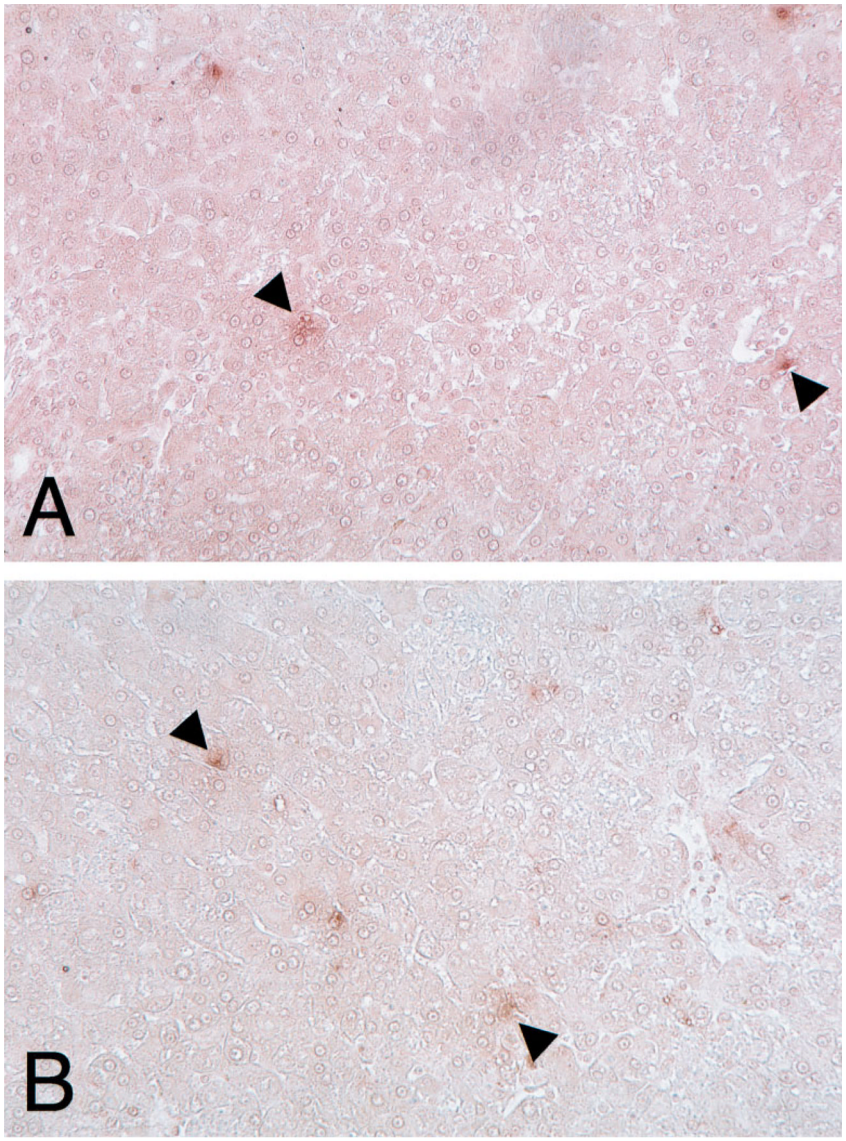

Fig. 4.

Immunohistochemistry of lymphocytic choriomeningitis virus (LCMV)-infected liver. Paraffin sections of Rh-iv3 (**A**) and Rh-iv6 (**B**) liver were stained with guinea pig anti-LCMV serum and immunoperoxidase-conjugated secondary antibodies. The red-brown foci (arrowheads) denote viral antigen. A,B, ×200.

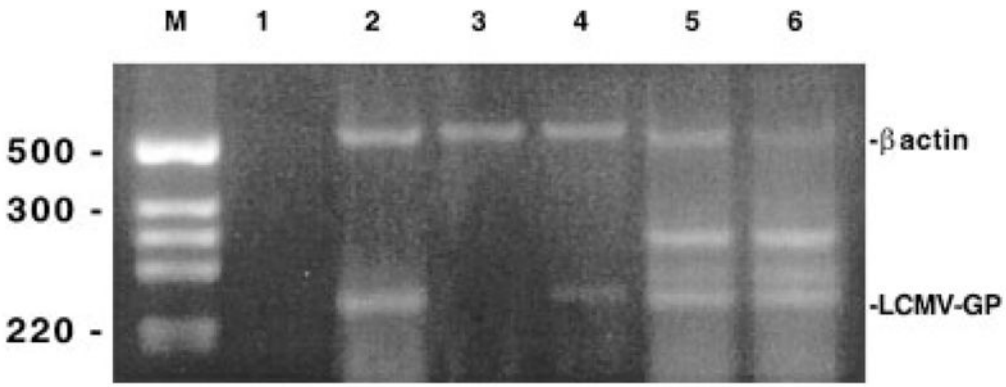

Fig. 5.

RT-PCR of RNA from Rh-igc, the rhesus monkey infected i.g. with 10^6 pfu lymphocytic choriomeningitis virus (LCMV)-Armstrong and euthanized 72 hr after infection. Total RNA was extracted from tissues and treated with DNase to ensure that the amplicons are derived from RNA and not DNA. **Lane M**, DNA molecular-weight markers; **lanes 1–6**, products of RT-PCR reactions: (1) in the absence of added nucleic acid, (2) LCMV-infected mouse splenic RNA for positive control, (3) pre-infection monkey PBMC RNA for negative control, (4) RNA from 72-hr PBMC from monkey Rh-igc, (5) 72-hr splenic RNA from Rh-igc, and (6) 72-hr stomach RNA from Rh-igc.

TABLE I

Clinical Signs and Body Temperature* During the Acute Phase of Disease

Monkey	Dose and route of inoculation	Day 0	Day 5	Day 7	Day 8	Day 9
Rh-iv3	10^3 i.v.	(101°F)	No signs (101°F)	Unkempt (103°F)	Unkempt (103°F) Listless	Unkempt (105°F) Listless Low food/water intake Orbital hemorrhaging
Rh-iv6	10^6 i.v.	(101°F)	Unkempt (103°F)	Unkempt (103°F)	Unkempt (104°F) Listless Low water intake	Unkempt (105°F) Diarrhea No food/water intake Orbital hemorrhaging
Rh-ig6a	10^6 i.g.	(101°F)	Unkempt (103°F)	Unkempt (102°F)	No signs (101°F)	No signs (101°F)
Rh-ig6b	10^6 i.g.	(101°F)	Unkempt (103°F)	Unkempt (102°F)	No signs (101°F)	No signs (101°F)
Rh-ig6c	10^6 i.g.	(101°F)	Euthanized 72 hr after inoculation			

* Normal rhesus macaque body temperature is 101–102°F. Body temperature is in parentheses.

J Med Virol. Author manuscript; available in PMC 2008 May 29.

TABLE II

Hematology Report on LCMV-WE-Inoculated Rhesus Macaques

	Rh-iv3			Rh-iv6			Rh-ig6a			Rh-ig6b		
	d0	**d7**	**d11**	**d0**	**d7**	**d12**	**d0**	**d7**	**d14**	**d0**	**D7**	**d14**
WBC, ths/μl	6.3	4.8	10.5	5.3	8.5	11.3	15.4	14.5	14.6	7.9	9.9	9.5
RBC, ths/μl	5.57	5.19	4.67	4.71	4.19	3.35	5.31	5.04	4.97	4.47	4.11	4.29
Hb, g/dl	13.6	12.4	11.3	11.8	10.7	8.6	12.9	12.5	12.2	11.5	10.9	11.2
HCT, %	41.8	38.2	34.4	37.5	32.8	26.2	40.0	38.5	38.2	5.2	23.4	34.1
MCV, fl	75.0	73.6	73.7	79.7	78.2	78.1	76.2	76.3	76.8	78.8	78.8	79.4
MCH, pg	24.4	23.9	24.2	25.1	25.5	25.7	24.3	24.8	24.5	25.7	25.8	26.1
MCHC, %	32.5	32.5	32.8	31.5	32.6	32.8	31.9	32.5	31.9	32.7	32.7	32.8
RDW, %	14.2	14.7	14.6	15.2	15.5	15.8	12.8	13.3	13.0	14.5	14.2	14.3
PLT, ths/μl	529	185[a]	87[a]	390	131[a]	43[a,b]	469	473	359	338	371	347
MPV, fl	8.9	11.5	9.6	10.4	12.4	12.4	9.9	10.2	10.6	10.2	9.8	10.3
Neutrophils, %	59.0	36.0	39.0	51.0	56.0	67.5	69	58	34	62	88	64
Lymphocytes, %	40.0	64.0	57.5	47.0	39.0	27.5	28	40	64	35	12	31
Monocytes, %	0.0	0.0	1.0	0.0	3.0	0.0	1.0	1.0	1.0	2.0	0.0	1.0
Eosinophils, %	0.0	0.0	0.0	0.0	0.0	0.0	2.0	0.0	1.0	1.0	0.0	4.0
Basophils, %	1.0	0.0	0.5	1.0	1.0	2.0	0.0	1.0	0.0	0.0	0.0	0.0

LCMV, lymphocytic choriomeningitis virus; d, day after infection (d0, d7, d14); WBC, white blood cells; RBC, red blood cells; Hb, hemoglobin; HCT, hematocrit; MCV, mean corpuscular volume (mean volume of erythrocytes counted in the sample); MCH, mean corpuscular hemoglobin (mean mass of hemoglobin in red cells); RDW, red cell distribution width; PLT, platelets; MPV, mean platelet volume.

[a] Below normal range for rhesus macaques.

[b] Giant platelets were noted.

TABLE III

Serum Blood Chemistries of LCMV-WE-Inoculated Rhesus Macaques

	Rh-iv3			Rh-iv6			Rh-ig6a			Rh-ig6b		
Analytes	**d0**	**d7**	**d11**	**d0**	**d7**	**d12**	**d0**	**d7**	**d14**	**d0**	**d7**	**d14**
Glucose, mg/dl	100	88	79	85	61	73	71	50	51	90	65	80
BUN, mg/dl	15	21	24	16	21	36	16	21	16	20	29	23
Creatinine, mg/dl	1.0	1.5	1.2	0.7	1.0	1.0	0.5	0.8	0.7	0.9	1.0	0.8
CK(CPK), mg/dl	405	678	1,490[a]	159	238	882	676	649	353	516	435	260
Cholesterol, mg/dl	155	190	136	142	110	64	130	137	153	130	137	153
Triglycerides, mg/dl	16	44	68	10	53	89	10	17	32	11	70	70
AST (SGOT), mu/dl	84	190[a]	642[a]	34	200[a]	1,422[a]	44	321[a]	52	63	52	56
LDH, mu/dl	202	1,022	1,669	206	727	3,792[a]	342	242	242	293	209	326
T bilirubin, mu/dl	0.2	0.2	0.6	0.2	0.2	1.1[a]	0.3	0.3	0.1	0.3	0.2	0.2
GGT, mu/dl	45	33	166[a]	43	42	238[a]	81	73	68	52	48	46
SGPT (ALT), mu/dl	26	5	587[a]	23	92[a]	646[a]	41	22	24	33	34	34
T protein, g/dl	7.1	5.7	4.5	6.6	6.2	5.1	7.0	6.7	6.8	6.8	6.6	6.2
AP, mu/dl	638	454	1,037[a]	212	139	217	638	580	594	170	149	160
Calcium, mg/dl	10.1	8.7	8.1	8.9	8.6	8.1	9.7	9.9	9.9	9.1	9.5	9.8
Phosphorus, mg/dl	6.4	5.9	3.7	8.9	8.6	8.1	5.9	6.8	5.8	4.2	5.1	4.4
Iron, μg/dl	161	132	269[a]	98	76	324[a]	61	60	69	130	93	141
Sodium, mmol/L	150	147	142	145	143	141	148	148	146	148	148	145
Potassium, mmol/L	3.7	3.3	3.4	3.3	2.9	2.5	3.4	3.3	3.5	3.5	3.5	3.7
Chloride, mmol/L	109	110	103	109	104	105	108	110	112	111	111	112

LCMV, lymphocytic choriomeningitis virus; d, day after inoculation (d0, d7, d14); BUN, blood urea nitrogen; CK (CPK), creatine kinase (creatine phosphokinase); AST (SGOT), aspartate aminotransferase; LDH, lactate dehydrogenase; T bilirubin, total bilirubin; GGT, γ-glutaminotransferase; SGPT (ALT), alanine aminotransferase; T protein, total protein; AP, alkaline phosphatase.

[a]Values that lie outside the normal range for rhesus macaques.

TABLE IV

Necropsy Findings for Rhesus Macaques Inoculated Intravenously (iv) With LCMV-WE

Tissues	Rh-iv3	Rh-iv6
Skin	Erythematous around eyes and dehydrated	Erythematous skin flaking on face, inner thigh, and upper arms
Lungs	Mild multifocal pulmonary edema; hemorrhage (red mottling) on lung surface	Moderate multifocal edema, mild alveolar histiocytosis; perivascular edema; 4–5-mm-diam hemorrhagic foci
Thymus	Severe diffuse depletion; scant foci of lymphocytes around the remaining Hassall's corpuscles	Severe diffuse depletion
Lymph nodes	Moderate multifocal lymphoid depletion; no normal follicles, sinus histiocytosis	Multifocal paracortical hyperplasia, a few normal follicles, sinus histiocytosis
Bone marrow	Moderate diffuse marrow depletion; M:E ratio 1:1	Severe diffuse marrow depletion; M:E ratio 1:2
Spleen	Red pulp moderately and diffusely congested	Red pulp moderately and diffusely congested
Brain	No significant lesions	A 1-cm area of hemorrhage in the subcutis of the parietal lobe
Buccal cavity	Few foci of necrotic cells in the striatum basale and stratum spinosum containing eosinophilic cytoplasm and pyknotic nuclei surrounded by a clear halo; scant multifocal lymphocytic infiltrates at the interface of mucosa and submucosa; salivary glands had mild multifocal lymphoplasmacytic sialoadenitis, and infiltrates of lymphocytes and plasma cells surrounding salivary ducts and, to a lesser, extent salivary glands	Multifocal acute stomatitis; foci of necrotic cells in stratum basale and stratum spinosum containing eosinophilic cytoplasm and pyknotic nuclei surrounded by a clear halo; scant multifocal infiltrates of lymphocytes and plasma cells at the interface of mucosa and submucosa
Heart	No significant lesion	The anterior surface of the right ventricle had a 0.5-cm opaque white plaque on the epicardium
Small intestine	Moderate multifocal lymphangiectasis	Moderate multifocal lymphangiectasis, villous congestion; diffuse transmural reddening with more severe bleeding in segments distal to stomach
Liver	Mild to moderate multifocal necrosis; minimal numbers of inflammatory cells; mild multifocal lymphoplasmacytic cholangiohepatitis	Mild to moderate multifocal necrosis; minimal numbers of inflammatory cells; mild multifocal lymphoplas-macytic cholangiohepatitis
Stomach	Mild multifocal mucosal hemorrhage	Mild regionally extensive lymphoplasmacytic gastritis
Bladder	Surface has mild scattered petechia, thick, gelatinous walls; moderate multifocal edema and mild mucosal hemorrhage; intraepithelial necrosis with minimal multifocal cystitis	Surface has mild scattered petechia
Kidney	No significant lesions	Moderate scattered epithelial cells with cytoplasmic eosinophilia in the cortical tubules; cytoplasm of these cells is usually clumped, and nuclei are shrunken, hyperchromatic

LCMV, lymphocytic choriomeningitis virus.

TABLE V

Necropsy Findings for Rhesus Macaques Inoculated by Gavage (i.g.) With LCMV-WE

Tissues	Rh-ig6a	Rh-ig6b
Skin	Mild erythyma around right orbit	No significant lesions
Lungs	No significant lesions	One section had alveoli filled with edema fluid, with no macrophages
Thymus	No significant lesions	No significant lesions
Lymph nodes	No significant lesions in inguinal and mediastinal nodes; sinuses of peripheral, axillary, and ileocecal nodes had numerous multifocally distributed macrophages containing cytoplasmic red-brown globular material	Moderate multifocal sinus histiocytosis; sinuses of peripheral, axillary, and ileocecal nodes had numerous multifocally distributed macrophages containing cytoplasmic red-brown globular material
Bone marrow	Normal M:E ratio 1:1	Normal M:E ratio 1:1
Spleen	Germinal centers mildly expanded by deposits of an amorphous eosinophilic material	Germinal centers mildly expanded by deposits of an amorphous eosinophilic material
Brain	No significant lesions	No significant lesions
Buccal cavity	No significant lesions	No significant lesions
Heart	Rare scattered infiltrates of lymphocytes and macrophages in sections from interventricular septum and left ventricle	A small fibrous adhesion was between the right ventrical epicardium and pericardium
Small intestine	Mild multifocal dilation of the lymphatics in the lamina propria	No significant lesions
Liver	No significant lesions	No significant lesions
Stomach	Mild multifocal subacute cholangitis of the gallbladder; moderate multifocal lymphoplasmacytic gastritis	Stomach showed signs of severe multifocal lymphoplasmacytic gastritis; the lamina propria contained a severe infiltrate of plasma cells and lymphocytes that moderately separated the glands; stomach lymphocytes occasionally formed follicle-like structures at the base of the lamina propria
Bladder	No significant lesions	No significant lesions
Kidney	No significant lesions	Scattered multinucleate cells in the medullary tubule epithelium
Uterus/cervix	Focus of adenomyosis	No significant lesions

LCMV, lymphocytic choriomeningitis virus.

TABLE VI

Virus Recovery From Plasma and Tissue Samples of LCMV-WE-Inoculated Rhesus Macaques

Monkey	Plasma pfu/ml[a]		Tissue pfu/g						Inf. Cnt.[b]	
	Day 7	Day 11	Spleen	Liver	Stomach	Colon	Lung	Hypothalmus	MLN	Spleen
Rh-iv3	7.5×10^4	1.0×10^6	1.1×10^7	5.5×10^5	1.0×10^6	1.6×10^6	5.0×10^5	8.3×10^5	0.5	4.3
Rh-iv6	2.0×10^5	1.2×10^7	7.3×10^7	1.0×10^8	1.0×10^6	1.0×10^7	8.9×10^6	6.3×10^5	1.0	1.6
Rh-ig6a	—	—	—	—	—	—	—	—	—	—
Rh-ig6b	—	—	—	—	—	—	—	—	—	—
Rh-ig6c	Euthanized 72 hr after inoculation (no pfu detected)									

LCMV, lymphocytic choriomeningitis virus; MLN, mesenteric lymph node.

[a] Plaque-forming units (pfu) were determined on Vero cell monolayers at six different dilutions. Results represent the mean viral titers from two titrations. Absence of detectable plaques is denoted by a dash (—).

[b] Infectious center (Inf. Cnt.) assays were done on Vero cell monolayers and were expressed as pfu per 10^3 monkey cells.

J Med Virol. Author manuscript; available in PMC 2008 May 29.

TABLE VII

Detection of Virion RNA in Plasma of Rhesus Macaques Infected With LCMV-WE

Monkey	Days after inoculation	RT-PCR (real-time), C_T[c]	
		GP primers	NP primers
Rh-iv3	−14	40.0	40.0
	0	40.0	40.0
	7	32.75–33.19[b]	30.90–31.18[b]
	11[a]	28.90–29.09[b]	25.00–25.53[b]
Rh-iv6	−14	40.00	40.00
	0	40.00	40.00
	7	28.75–29.21[b]	26.37–26.67[b]
	11[a]	27.30–27.86[b]	21.72–22.69[b]
Rh-ig6a	−14	40.00	40.00
	0	40.00	40.00
	7	40.00	40.00
	14	39.15–40.00	40.00
	21	35.91–36.31	34.86–36.47[b]
	28	37.34–40.00[b]	38.40–40.00
Rh-ig6b	−14	40.00	40.00
	0	40.00	40.00
	7	40.00	40.00
	14	38.08–40.00	40.00
	21	37.85–40.00[b]	38.40–40.00
	28	40.00	40.00

LCMV, leukocyte choriomeningitis virus; RT-PCR, reverse transcription-polymerase chain reaction.

[a] Died with hemorrhagic manifestations.

[b] Positive for viral nucleic acid.

[c] Samples with C_T of < 36 were positive in nested RT-PCR assays, where amplicons could be visualized on gels after ethidium bromide staining.